Optimization of the Layout of the ITER ICRF Antenna Port Plug and its Performance Assessment

M. Vrancken, F. Durodié, P. Dumortier, D. Lockley, F. Louche et al.

Citation: AIP Conf. Proc. **1406**, 61 (2011); doi: 10.1063/1.3664929
View online: http://dx.doi.org/10.1063/1.3664929
View Table of Contents: http://proceedings.aip.org/dbt/dbt.jsp?KEY=APCPCS&Volume=1406&Issue=1
Published by the American Institute of Physics.

Optimization of the Layout of the ITER ICRF Antenna Port Plug and its Performance Assessment

M. Vrancken[a], F. Durodié[a], P. Dumortier[a], D. Lockley[c], F. Louche[a], A. Messiaen[a], R. Maggiora[b], D. Milanesio[b], M.P.S. Nightingale[c], P. Tigwell[c], M. Van Schoor[a], D. Wilson[c] and the CYCLE Team[a,b,c,d,e]

[a] LPP/ERM-KMS, Association EURATOM-Belgian State, Brussels, Belgium
[b] Associazione EURATOM-ENEA, Politecnico di Torino, Torino, Italy
[c] EURATOM/CCFE Fusion Association, Culham Science Centre, UK
[d] IPP-MPI, EURATOM-Assoziation, Garching, Germany
[e] Association EURATOM-CEA, DSM/IRFM, Cadarache, France

Abstract. The ITER ICRF antenna's coupled power to plasma is determined not only by the plasma scrape-off layer profiles and shaping of the front strap array, but also by assuring optimal excitation of the array by the overall layout of the feed network and the detailed shaping of the RF components therein. This paper describes the optimization of the feed network layout inside the port plug with 4-port junction, vacuum window and service stub components under RF, thermo-mechanical, manufacturing and assembly constraints.

Keywords: ICRF, antenna, ITER.
PACS: 52.50.Qt, 52.50.Fa

INTRODUCTION

The RF performance of the proposed ITER ICRF antenna is in first instance determined by the plasma Scrape-Off Layer (SOL) profiles and the geometry of the antenna array front face [1]. Additionally, the best achievable excitation of the array follows from optimizing the overall layout of the feed network and the details of the RF surfaces therein. Thermo-mechanical cooling, strength and assembly considerations are also taken into account. A sideview of the TransMission Line (TML) component layout feeding a poloidal triplet of straps is shown in Figure 1 and is repeated 8 times as shown in Figure 3. The layout is determined by the length

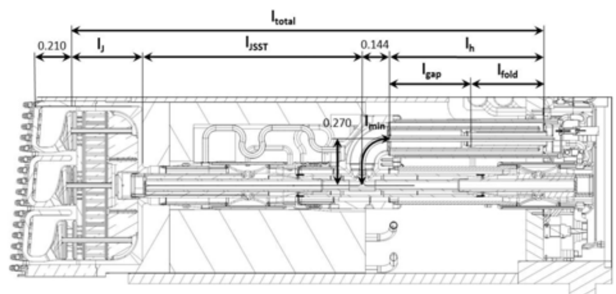

Figure 1: Side view of 1/8 of the ITER ICRF antenna with main dimensions (units [m]): length of 4-port junction l_J, distance l_{JSST} to service stub of length $l_{SST}=l_{min}+l_h+l_{fold}$ with inward fold length l_{fold} and remaining gap length $l_{gap}>0$.

Radio Frequency Power in Plasmas
AIP Conf. Proc. 1406, 61-64 (2011); doi: 10.1063/1.3664929

of the 4-Port Junction (4PJ) l_J, the distance l_{JSST} to the T-point connection with the Service Stub (SST) and its length l_{SST}. The overall length is limited to l_{total}=2.721m, such that the ~$\lambda_{midband}$/4 SST can be fitted with an inward fold of length l_{fold} if a gap distance $l_{gap}>0$ remains.

4-PORT JUNCTION OPTIMISATION

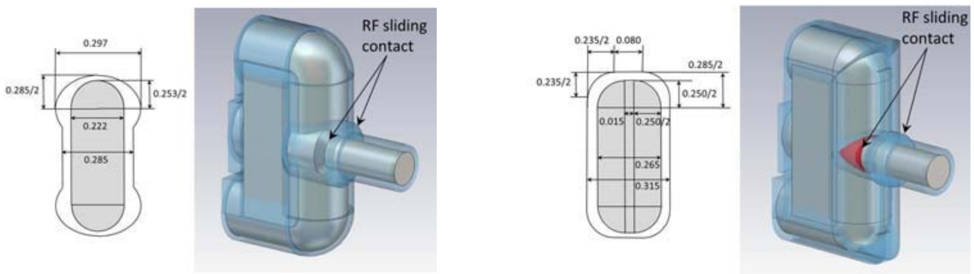

(a) (b)

Figure 2: Cross section (units [m]) and 3D view of 4-Port Junctions with off-set feed line and sliding RF contact with (a) elliptic shaping (b) rectangular/circular shaping of inner conductor and outer cavity, for $max(|E_{//}|)$=3kV/mm and $max(|E_{\perp}|)$=2.5kV/mm electric field control.

A previous "trident" 4PJ design consisted of an assembly of 3 coaxial lines [2], and an average 1.5kV/mm electric field between inner and outer conductor. However, the outer housing mechanical "clamshell" assembly is problematic, whilst electric field specifications have evolved into $max(|E_{//}|)$=2kV/mm and $max(|E_{\perp}|)$=3kV/mm in torus vacuum and $max(|E|)$=3kV/mm in antenna private vacuum on all RF surfaces [3]. Cooling and assembly is strongly improved by joining the 3 lines into a single TML as in Figure 2(a) which retains the in-phase excitation of the 3 straps. Some coupled power performance loss due to the modified characteristic impedance of the central part is more than compensated by the increased allowable electric field inside the junction. The elliptic shaping of the outer surface in Figure 2(a) to locally control $max(|E_{//}|)$ raises problems with stress, cooling channel distribution and manufacturing. Figure 2(b) shows a 4PJ with circular/rectangular shaped cross section, avoiding outer double curved surfaces and improved integration of the sliding RF contact of the off-set feed line "into" the junction inner.

VACUUM WINDOW AND SERVICE STUB

CST MicroWave Studio® [4] (MWS) modeling of VaCuum Window (VCW) and SST are performed to capture non-negligible 3D effects. The VCW was reduced to 90% of its original size [5] and the ceramic's curvature increases its strength. Initial VCW modeling only incorporated a difference between physical and electrical length of Δl_{VCW}=-0.084m, while an improved model consists of a 3+1+3-section TML model with varying characteristic impedance Z_{ci} and propagation constants β_i to account for the varying position of the ceramic. The T-junction connects the 15Ω SST to the 20Ω TML by a conical transition (inner conductor only) and can be sufficiently accurately modeled with length corrections Δl_{SST}=+0.0830m, Δl_{JSST}=+0.004m, while the folding and short have appear to behave near-perfect. The diameter reduction at the fold creates an electric field concentration that needs to remain below 3kV/mm.

FULL ARRAY COUPLED POWER OPTIMISATION

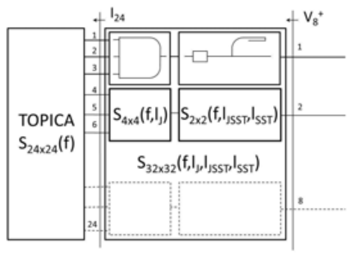

Figure 3: Circuit block diagram for coupling antenna array S_{24x24}- to feed network S_{32x32}-matrix with amplitude and phase excitations V_8^+ and antenna strap currents I_{24}.

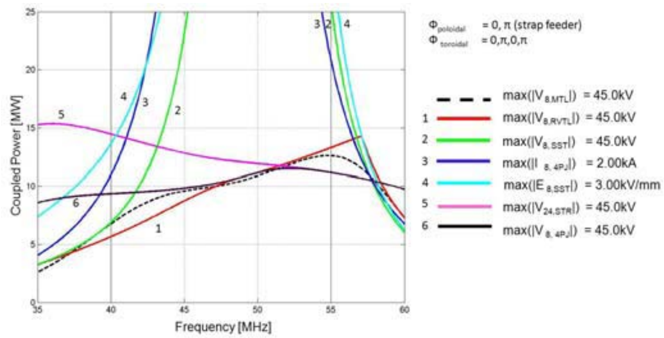

Figure 4: Total coupled power for given poloidal and toroidal phasing as a function of frequency with $max(|V_{8,MTL}|)$=45kV is additionally constrained by limits on RF quantities inside the feed network to the lowest of the curves shown. 4PJ of Figure 2(a) with l_J=0.483m, l_{JSST}=1.350m+Δl_{JSST} +Δl_{VCW}, l_{SST}=1.590m+Δl_{SST}.

To optimize the full antenna's power coupled to plasma, a TOPICA [2] S_{24x24} matrix, calculated with an ITER April 2010 provided "low density" edge profile (pessimistic case), is combined with 8 sets of S_{4x4} and S_{2x2} matrices to determine the lengths l_J, l_{JSST}, l_{SST}. Excitation of the Main Transmission Line (MTL) feed points with 8 complex forward voltages V_8^+ will produce a current distribution at the strap input ports $I_{24}=Y_{24x8}.V_8^+$, with Y_{24x8} constructed from S_{4x4} and S_{2x2} matrices. The best excitation to approximate a current distribution I_{24}^P (desired poloidal and toroidal phasing P) can be obtained from a (complex) least square approximation

$$V_{8,LSQ}^+ = (Y_{24x8}{*}^T . Y_{24x8})^{-1} . Y_{24x8}{*}^T . I_{24}^P$$

with complex conjugate * and transpose ^{T}. The coupled power $\sum Re(P_8)$ is obtained by scaling the maximum (total) voltage on the 8 (infinitely long) MTLs to $max(|V_{8,MTL}|)$=45kV. Additional RF quantities between straps and MTL feed points

- $max(|V_{24,STR}|)$, voltage limit on STRap (STR) feeders
- $max(|V_{8,4PJ}|)$, voltage limit inside the 4PJ
- $max(|V_{8,RVTL}|)$, voltage limit on the Removable Vacuum TL's (RVTL)
- $max(|V_{8,SST}|)$, voltage limit on SST's
- $max(|E_{8,SST}|)$, electric field limit inner of SST bends
- $max(|I_{8,4PJ}|)$, current in sliding contacts between RVTL and 4PJ

also need to be limited below the values in the legend of Figure 4, such that the actual achievable coupled power is the "lower envelope" of the set of depicted curves. The exact position of the limitations is adjusted through the choice of l_J, l_{JSST} and l_{SST}.

Figure 5 shows the resulting performance for all expected array phasings for the improved 4PJ of Figure 2(b) and VCW 3+1+3-section TML model. A slight shortening of l_{JSST} allows a shorter SST inward folded part which avoids the $max(|E_{8,SST}|)$ limitation becoming more constraining than the $max(|I_{8,4PJ}|)$, $max(|V_{8,SST}|)$ constraints in the high frequency range. A further investigation into the required accuracy with which the optimum excitations $V_{8,LSQ}^{+}$ need to be realized to retain predicted performance will generate RF amplitude/phase accuracy specifications for the feed network outside the port plug [6] and the RF generators.

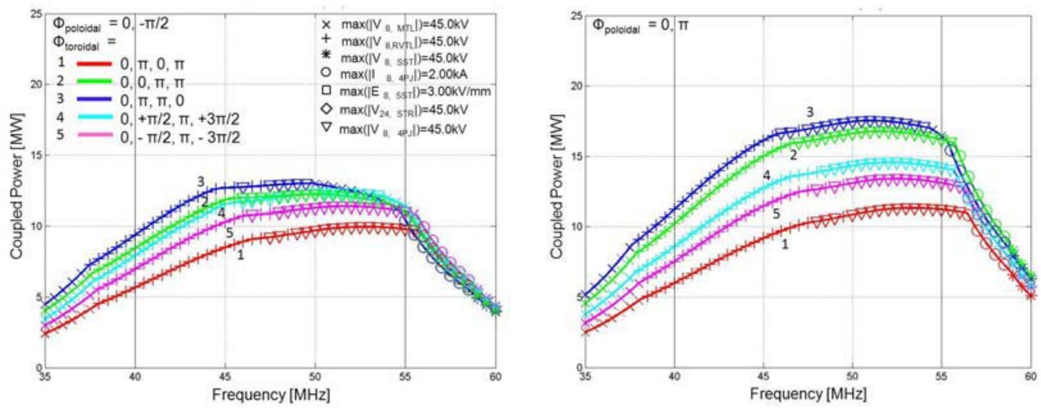

(a) (b)

Figure 5: Antenna array coupled power as a function of frequency for poloidal phasing (a) (0,-π/2) (b) (0,π) as delimited by several RF quantities for the rectangular/circular junction of Figure 2(b) with l_J=0.433m, l_{JSST}=1.175m+Δl_{JSST}, and l_{SST}=1.630m+Δl_{SST} and 3+1+3 section TML model of the VCW, leaving a gap of length l_{gap}=0.571m.

CONCLUSIONS

This paper has described the optimization of the power coupling capability of the ITER ICRF antenna, starting from the presently predicted strap array to plasma RF coupling as based on present SOL profiles, by shaping the layout and components of the feed network inside the port plug and incorporating RF, thermo-mechanical, manufacturing and assembly constraints. Excluding significant changes in the presently assumed boundary conditions, any further necessary corrections are expected to remain within close tolerance from the presently proposed geometry.

ACKNOWLEGDMENTS

The project F4E-2009-GRT-026 has been funded with support from Fusion from Energy. This publication reflects the views only of the author, and Fusion for Energy cannot be held responsible for any use which may be made of the information contained herein. The views and opinions expressed herein do not necessarily reflect those of the ITER Organization.

REFERENCES

[1] F. Louche et al., These Proceedings.
[2] Messiaen et al., AIP Conf. Proc, **1189**, 269-272 (2009).
[3] ITER_D_3XWCT9, ITER Design Review, answer to ITER_D_34WL62 - # 04 Chit.
[4] CST GmbH, CST Microwave Studio®, User Manual (2008)
[5] C. Hamlyn-Harris et al., Fus. Eng. Des., **84**, 887-894 (2009)
[6] D. Grine et al., These Proceedings.